

# Development and characterization of single gap glass RPC

Manisha\*, V. Bhatnagar, J.S. Shahi, J.B. Singh

*Department of Physics, Panjab University,  
Chandigarh-160014, India.*

## Abstract

India-based Neutrino Observatory (INO) facility is going to have a 50 kton magnetized Iron CALorimeter (ICAL) detector for precision measurements of neutrino oscillations using atmospheric neutrinos. The proposed ICAL detector will be a stack of magnetized iron plates (acting as target material) interleaved with glass Resistive Plate Chambers (RPCs) as the active detector elements. RPC is a gaseous detector made up of two parallel electrode plates having high bulk resistivity like that of float glass and bakelite. For ICAL detector, glass is preferred over bakelite as it does not need any kind of surface treatment to achieve better surface uniformity and also the cost of associated electronics is reduced. Under detector R&D efforts for the proposed glass RPC detector, we have fabricated glass RPCs of 1m X 1m dimension procuring glass of ~ 2 mm thickness from one of the Indian glass manufacturers (Asahi). In the present paper, we report the characterization of RPC based on the leakage current study. Pulse width optimization is also carried out for the study of muon detection efficiency and noise rate with varying gas compositions.

Keywords : INO, ICAL, RPC, Leakage current, Efficiency

---

\* Corresponding author : manisha@pu.ac.in

## 1. Introduction

India-based Neutrino Observatory (INO) [1] is the proposed underground facility with an overburden of  $\sim 1$  km to be built at Pottipuram in Bodi West hills in the Western Ghats of India. ICAL detector is one of the biggest atmospheric neutrino detectors which will be established at the INO site. ICAL will be having three modules with dimensions of  $\sim 48$  m X  $16$  m X  $14.5$  m. Each ICAL module will be a stack of 151 layers of iron plates (5.6 cm thick) magnetized with an average magnetic field of  $\sim 1.5$  T. These iron layers will be interleaved with  $\sim 10,000$  glass RPCs (2 m X 2 m) in each module [2]. The primary goal of INO-ICAL is to improve significantly the measurements of neutrino oscillation parameters as compared to the earlier measurements [3, 4]. RPCs [5] are gaseous detectors (pioneered during 1980s) made up of two parallel electrode plates having high bulk resistivity similar to those of glass and bakelite. These detectors have two pick-up panels based readout system. The pick-up panels are placed orthogonally on each side of RPC gap, to extract the information about X and Y coordinates of the passage of charged particle through RPC. As ICAL detector will use  $\sim 30,000$  glass RPCs [7], therefore it is necessary to make dedicated efforts for their characterization. In the present paper, we report the RPC leakage current studies with different gas compositions, optimization of pulse width, muon detection efficiency and noise rate studies with the optimized pulse width values. Uniformity studies for the detection efficiency and noise rate at different locations of the RPC are also reported.

## 2. Fabrication of the glass RPC

Here, we briefly describe the fabrication process of glass RPC, which has been reported in detail by Santonico et al. [5]. Two glass plates having dimensions of 1 m X 1 m X 2 mm are used to make RPC electrodes. These plates are kept apart by polycarbonate button spacers having 10 mm diameter and 2 mm thickness to maintain uniform separation of 2 mm between the plates. Firstly glass plates are well cleaned with distilled water and subsequently with alcohol. Polycarbonate edge spacers (used to seal the glass RPC gas gap) are glued on one of the glass plates (along with gas nozzles). Once these glued edge spacers are dried enough, button spacers are glued with the help of mylar template on this glass plate. Then upper glass plate is glued carefully by gently placing it on the attached button spacers on the lower glass plate. Glass RPC gas gap is first subjected to gas leak test. Once gas leak rate ( $dP/dt$ ) is estimated, then it is subjected to spacer test. Spacer test is performed by gently pressing all the glued button spacers with thumb pressure. As button spacer is pressed, change in pressure is seen in the form of a peak. If any of the peaks overshoots, it means corresponding button spacer is popped up and is not glued with glass plates. The corresponding plots of leak test and spacer test are shown in Figure 1. Leak rate is estimated to be  $\sim 10^{-4}$  millibar/second. Number of peaks in the spacer test plot correspond to the number of button spacers glued between the two glass plates. Both the outer sides of gas gap are coated with graphite by spraying the graphite mixed using spray gun. Surface resistivity measurements of the graphite coated glass RPC gap are performed along both X and Y dimensions. These results are shown as contour plots in Figure 2. All the measured resistivity values have been found to be in the range 0.1 – 0.5  $M\Omega/\square$ . Final assembly of the RPC is done by attaching two pick-up panels on both the sides (each one for X and Y) to the graphite coated surfaces of RPC gap using kapton tape. Pick-up panels are made up of thin copper foils pasted on one side of the plastic honeycomb structure and the aluminium ground plane. Each pick-up panel has 32 strips etched out of copper foils having width 2.8 cm. Distance between two adjacent strips is 2

mm. For insulation purpose, mylar sheets are used between the pick-up panel and the graphite coated RPC gas gap.

### 3. Cosmic ray muon telescope setup

A cosmic ray muon telescope setup is used for the characterization of assembled glass RPC. The telescope assembly consists of 4 scintillator paddles marked as SP1, SP2, SP3 and SP4. The paddles SP1 and SP2 are placed below the assembled RPC (parallel to the X readout pick-up panel), SP3 and SP4 are placed above as shown in Figure 3. Two scintillator paddles SP1, SP2 have the dimensions of 20 cm X 84.5 cm. Other two scintillator paddles SP3, SP4 which decide the size of the telescope coincidence window have the dimensions of 2.8 cm X 34.5 cm. This way,

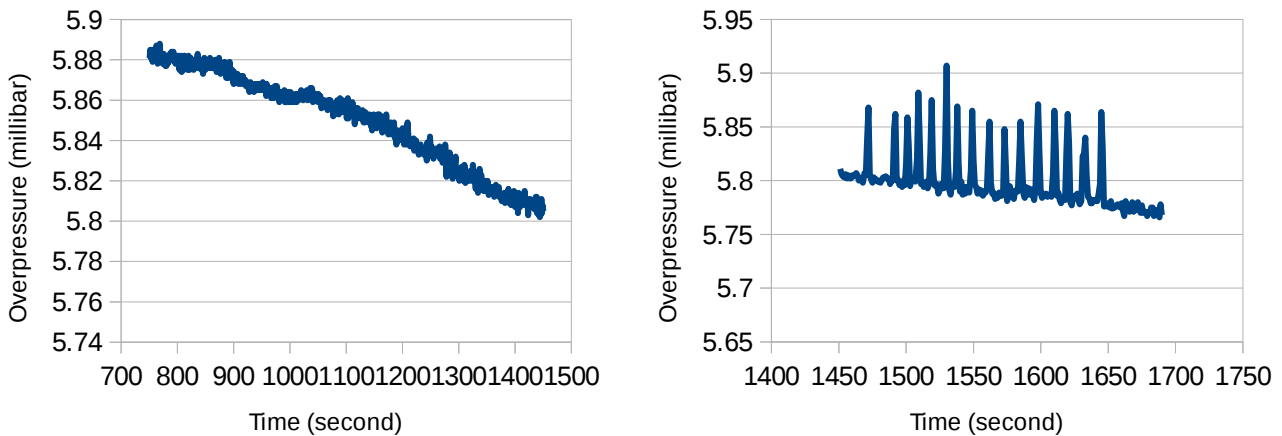


Figure 1: Leak test plot (left), spacer test plot (right) for the glass RPC gap.

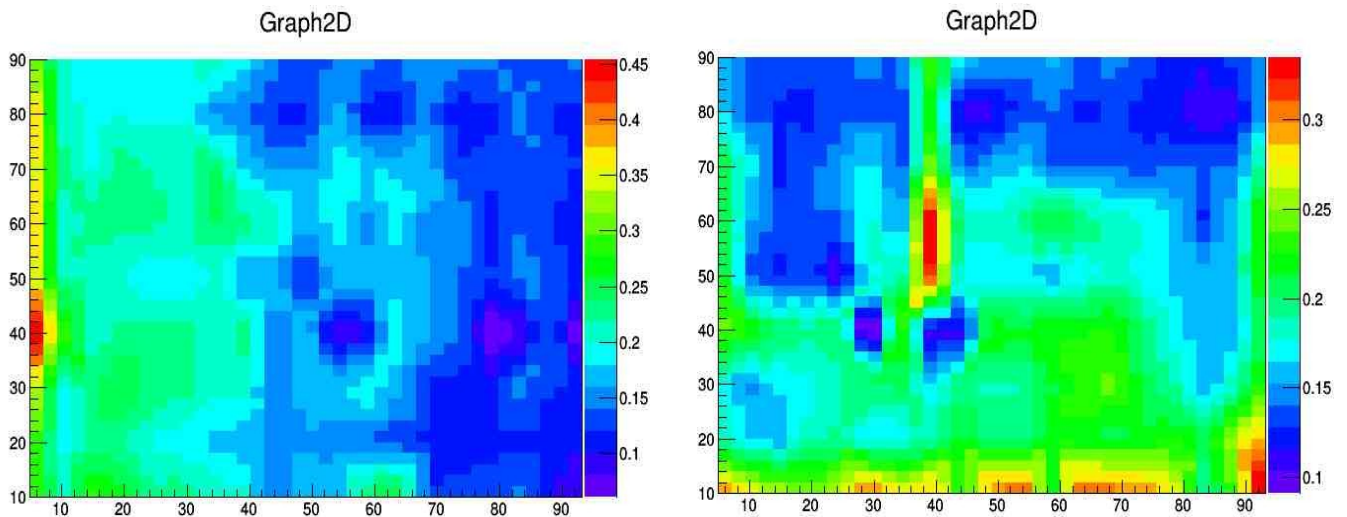


Figure 2: Contour plots of horizontal resistivity measurements (left), vertical resistivity measurements (right). Scale on the right side of each plot shows the resistivity values in MΩ. Glass dimensions along X and Y axes are in cm.

the size of telescope window available is 2.8 cm X 19 cm, which matches with the readout

strip width of the RPC. A schematic diagram of this telescope assembly is shown in Figure 3. A discriminated ANDed (4 fold coincidence) signal of these 4 scintillator paddles SP1, SP2, SP3 and SP4 is considered as the master trigger for RPC testing. Master trigger is put in coincidence with RPC strip signal, which forms 5 fold coincidence trigger. For the present study, fixed values of threshold are used which is 30 mV for scintillator paddles and 10 mV for RPC. Further for the characterization of RPC, we have used NIM and CAMAC based Data Acquisition (DAQ) system. Counts are recorded using a scalar unit for a time span of 10 minutes at regular intervals during pulse width optimization for efficiency and noise rate studies. Figure 4 shows block diagram of such a setup.

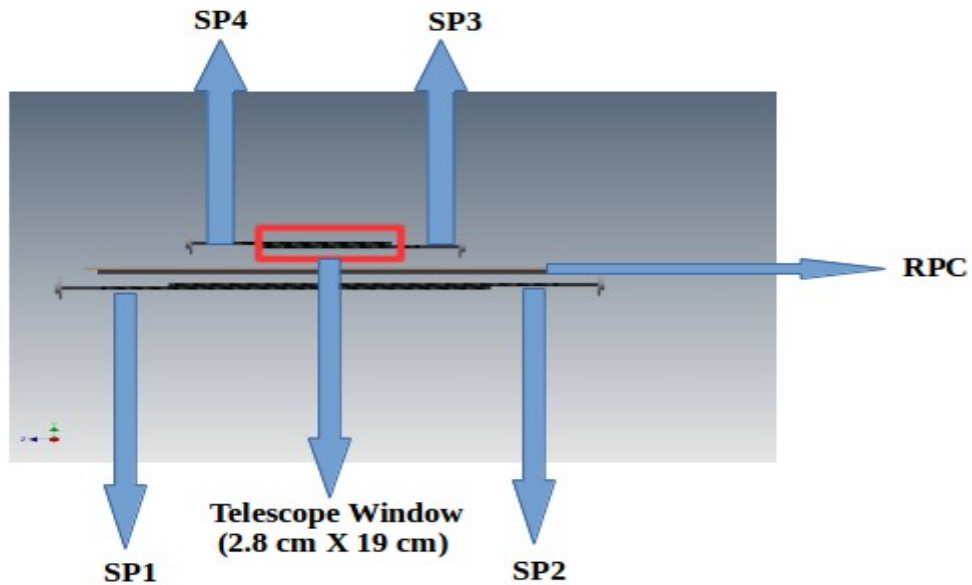


Figure 3: Cosmic ray muon telescope layout for the RPC testing.

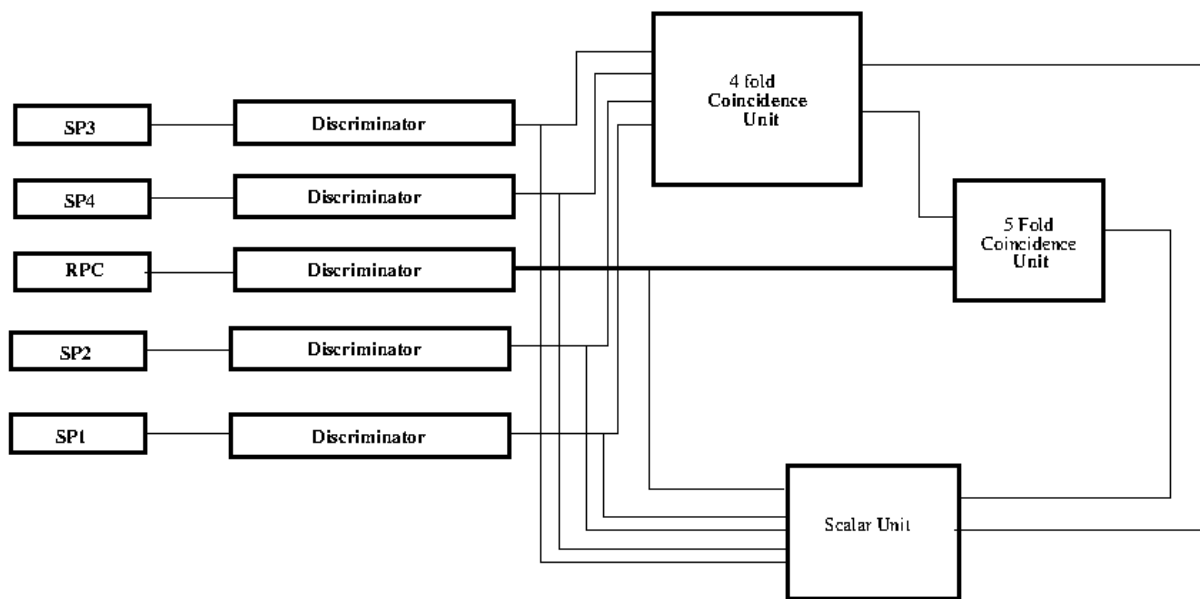


Figure 4: Block diagram of the cosmic ray muon telescope setup.

Delay induced due to the signal (analog and digital) carrying cables is taken care by adjusting the cable lengths.

#### 4. Detector Characterization

The VI characteristics of a RPC detector comes from the variation of leakage current (I) vs. applied voltage (V) for different gas operating compositions (as mentioned in Table 1). The VI characteristics are the base benchmark for optimizing the operating gas composition and pulse width. These optimized pulse width values are used further in the characterization of RPC. Efficiency and noise rate studies are performed - to check performance of the RPC and extent of operational uniformity. More details are given in following subsections. For all the reported studies, gas flow rate is kept 1 LPH (liter per hour). Laboratory ambient conditions are monitored round the clock and kept under control with temperature at 20–21°C, the relative humidity within 32-36% . Another important step, as part of the characterization process RPC gas gap is extensively flushed with nitrogen to remove any residual traces of humidity [8].

Sr. No.	Freon (R134A)	Isobutane (C <sub>4</sub> H <sub>10</sub> )	SF <sub>6</sub>	Argon(Ar)
1 <sup>st</sup> Composition	95.2 %	4.5 %	0.3 %	-
2 <sup>nd</sup> Composition	95.5 %	4.5 %	-	-
3 <sup>rd</sup> Composition	100 %	-	-	-
4 <sup>th</sup> Composition	-	-	-	100 %
5 <sup>th</sup> Composition	62 %	8 %	-	30 %

Table 1: Different compositions of the gases R134A, SF<sub>6</sub>, Ar, C<sub>4</sub>H<sub>10</sub> used for the RPC characterization.

##### 4.1 Leakage current

For selecting the optimized gas composition, the variation of leakage current (I) vs. RPC operating voltage (V) is measured for various gas compositions (Table 1). CAEN SY2527 (Universal Multichannel High Voltage Power Supply) is used for providing high voltage to the RPC electrodes. The variation of leakage current vs. voltage is shown in Figure 5. 1<sup>st</sup> gas composition clearly shows the minimum leakage current as SF<sub>6</sub> has quenching effect and the maximum leakage is seen for the 3<sup>rd</sup> gas composition as Freon has very high primary ionization [7]. Further we see from Figure 5 that the 2<sup>nd</sup> gas composition is also good for operating the RPC with low leakage current, therefore to operate the RPC with the small leakage current, we use the 1<sup>st</sup> and the 2<sup>nd</sup> gas compositions for the further characterization studies.

##### 4.2 Pulse width optimization

For making coincidence measurements, it is necessary to optimize all the pulse shape parameters those affect determination of the coincidence electronically and pulse width of the signal pulse is one such parameter. For better coincidence, besides pulse width, the minimum overlap required by the electronic pulses must be taken into account [8].

Therefore the pulse width optimization is performed for the four scintillator paddles (SP1, SP2, SP3, SP4) as well as for the RPC using the fixed values of threshold i.e. 30mV for the scintillator paddles and 10mV for the RPC. One pulse width value is fixed at a time, other one is varied either for the RPC or for the scintillator paddles (which constitute 4 fold coincidence). To optimize these two pulse width values, we perform the efficiency and noise rate studies of the RPC for various pulse width combinations as listed in Table 2. The efficiency and noise rate distributions for various pulse width combinations are shown in Figure 6. The RPC Efficiency is estimated as the ratio of 5 fold coincidence trigger to the total number of 4 fold master trigger. Further, the RPC noise rate is defined as the individual count rate of the RPC above an operating threshold. The efficiency is found to be the maximum for the 1<sup>st</sup> combination. Though the noise rate corresponding to the 4<sup>th</sup> combination is the minimum but the corresponding efficiency values were lower. Therefore, we have used the pulse width values of the 1<sup>st</sup> combination for further studies as this combination provides the maximum efficiency and comparatively lower noise rate.

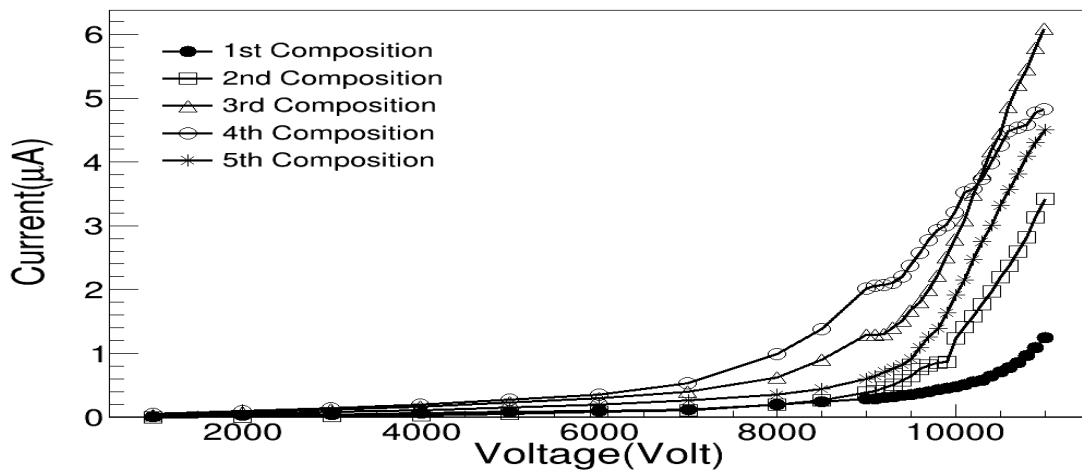


Figure 5: Leakage current vs. voltage characteristics for the different gas compositions.

Sr. No.	Scintillator pulse width (4 fold)	RPC pulse width
1 <sup>st</sup> Combination	60 ns	40 ns
2 <sup>nd</sup> Combination	75 ns	40 ns
3 <sup>rd</sup> Combination	70 ns	50 ns
4 <sup>th</sup> Combination	70 ns	60 ns

Table 2: Different combinations of pulse width values.

### 4.3 Efficiency and noise rate

For the 1<sup>st</sup> and the 2<sup>nd</sup> gas compositions as mentioned in Table 1, the efficiency and noise rate studies are performed for various readout strips of the RPC using the optimized pulse width obtained in previous section i.e. 40 ns for the RPC and 60 ns for the scintillator paddles. The efficiency and noise rate studies of 4<sup>th</sup>, 11<sup>th</sup>, 17<sup>th</sup>, 23<sup>rd</sup> and 29<sup>th</sup> strips are

shown in Figure 7-11 respectively. The efficiency of all the above mentioned strips of the RPC is  $\sim 96-97\%$  for both the 1<sup>st</sup> and 2<sup>nd</sup> gas compositions, which is not much affected by the observed noise rate in the range  $9-18 \text{ Hz/cm}^2$ . For all the tested RPC strips, efficiency increases significantly after 9000 V and reaches the plateau value corresponding to  $\sim 96-97\%$  from 9700 V-9800 V. An exponential increase is seen in the noise rate after 9000 V for all the RPC strips except 17<sup>th</sup> strip. Some unexpected fluctuations are observed in the noise rate of 17<sup>th</sup> strip, the statistical fluctuations can be one of the possible reasons for it.

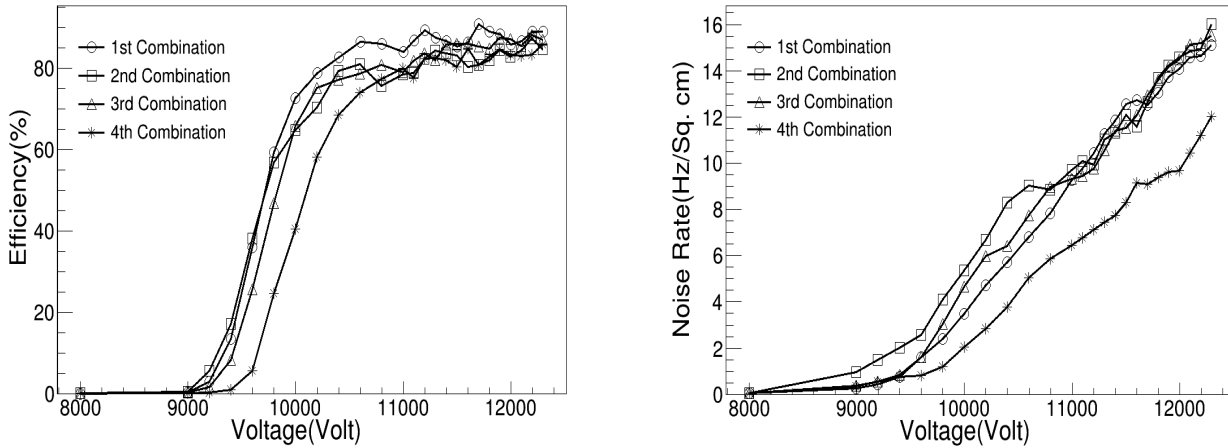


Figure 6: Efficiency vs. voltage characteristics (left), noise rate vs. voltage characteristics (right) for different combinations of the pulse width values.

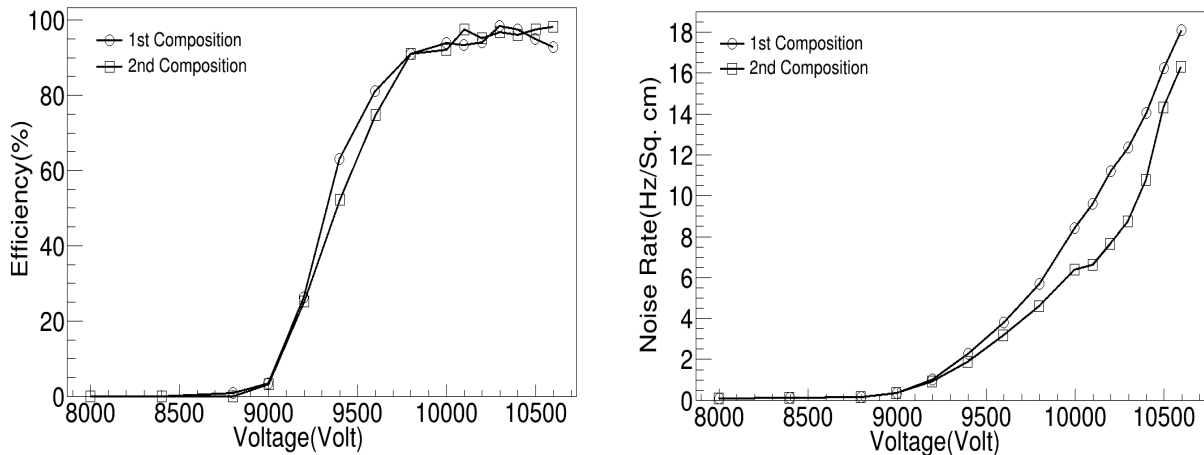


Figure 7: Efficiency vs. voltage characteristics (left), noise rate vs. voltage characteristics (right) for 4<sup>th</sup> strip.

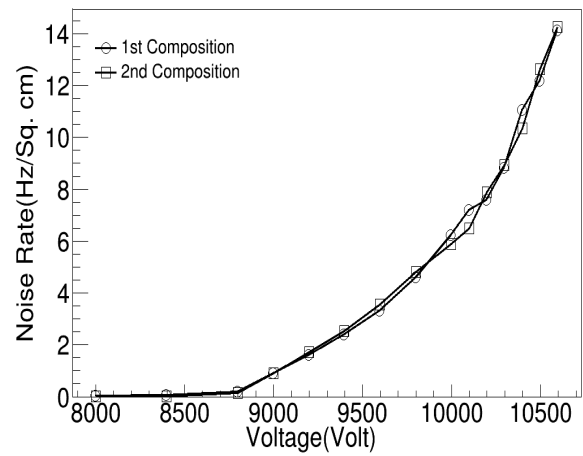
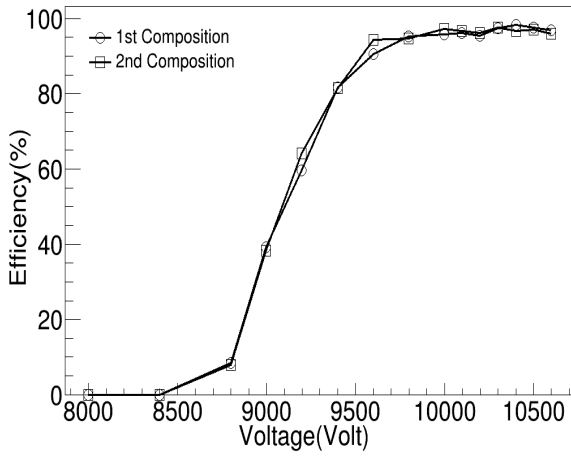


Figure 8: Efficiency vs. voltage characteristics (left), noise rate vs. voltage characteristics (right) for 11<sup>th</sup> strip.

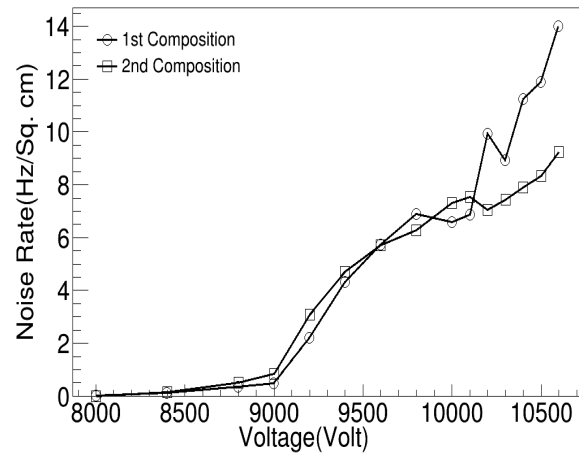
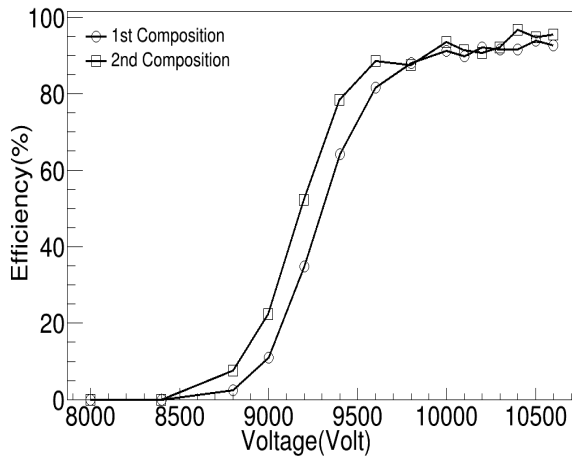


Figure 9: Efficiency vs. voltage characteristics (left), noise rate vs. voltage characteristics (right) for 17<sup>th</sup> strip.

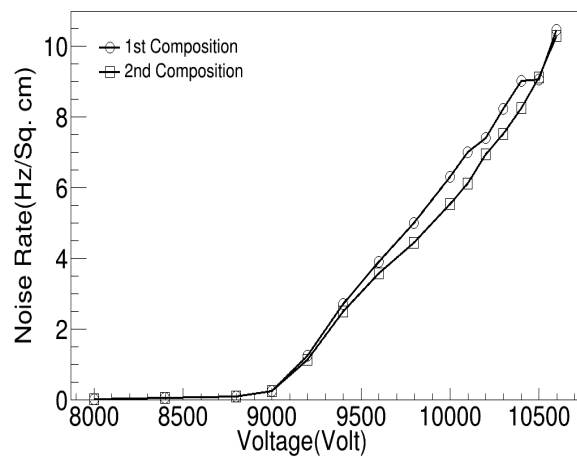
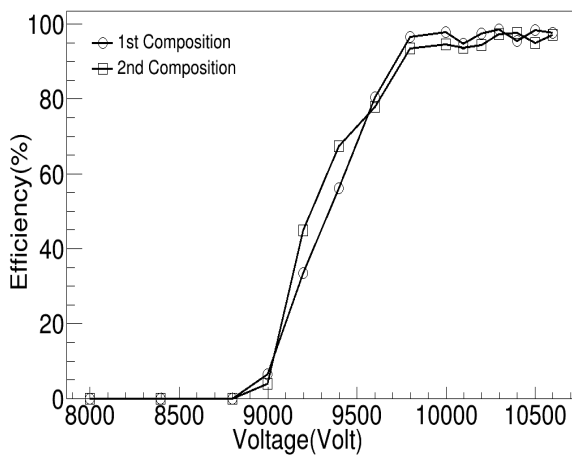


Figure 10: Efficiency vs. voltage characteristics (left), noise rate vs. voltage characteristics (right) for 23<sup>rd</sup> strip.

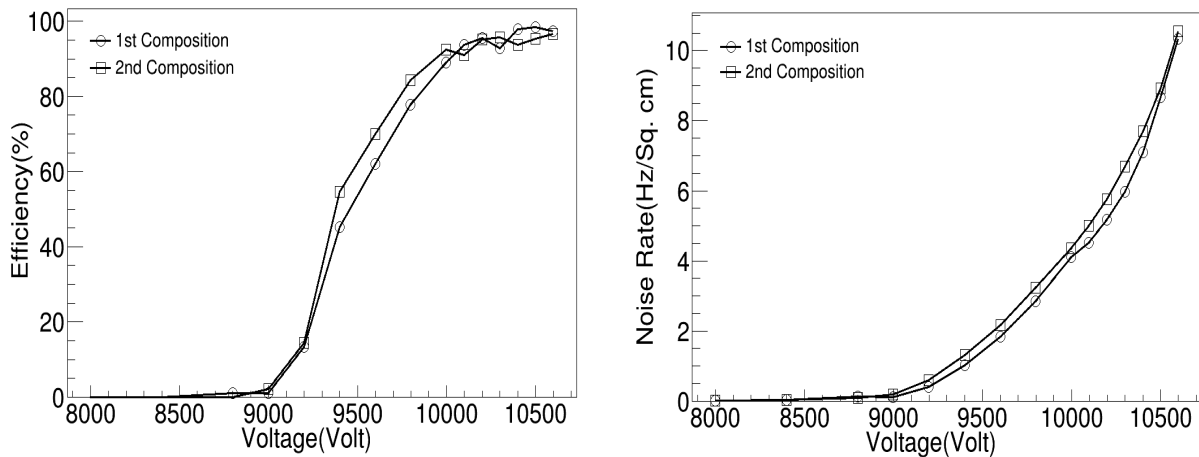


Figure 11: Efficiency vs. voltage characteristics (left), noise rate vs. voltage characteristics (right) for 29<sup>th</sup> strip.

#### 4.4 Uniformity studies

To test uniformity in the efficiency and the noise rate throughout the RPC for the 1<sup>st</sup> and 2<sup>nd</sup> gas compositions, we perform the efficiency and noise rate studies at 5 different locations corresponding to 5 different strips (4<sup>th</sup>, 11<sup>th</sup>, 17<sup>th</sup>, 23<sup>rd</sup> and 29<sup>th</sup>) of the RPC using the optimized pulse width values. In addition to this, discriminator threshold values are kept fixed as mentioned earlier (Section 3). The uniformity studies plots are shown in Figures 12, 13 respectively. For the 1<sup>st</sup> gas composition, the efficiency for these strips is  $\sim 98\%$  and noise rate is in the range of  $\sim 10\text{--}18 \text{ Hz/cm}^2$ . For the 2<sup>nd</sup> gas composition, the efficiency is in the range of  $\sim 96\text{--}98\%$  and the noise rate is in the range of  $\sim 10\text{--}16 \text{ Hz/cm}^2$ . Thus, we have observed consistent results for the uniformity in the efficiency and noise rate throughout the RPC.

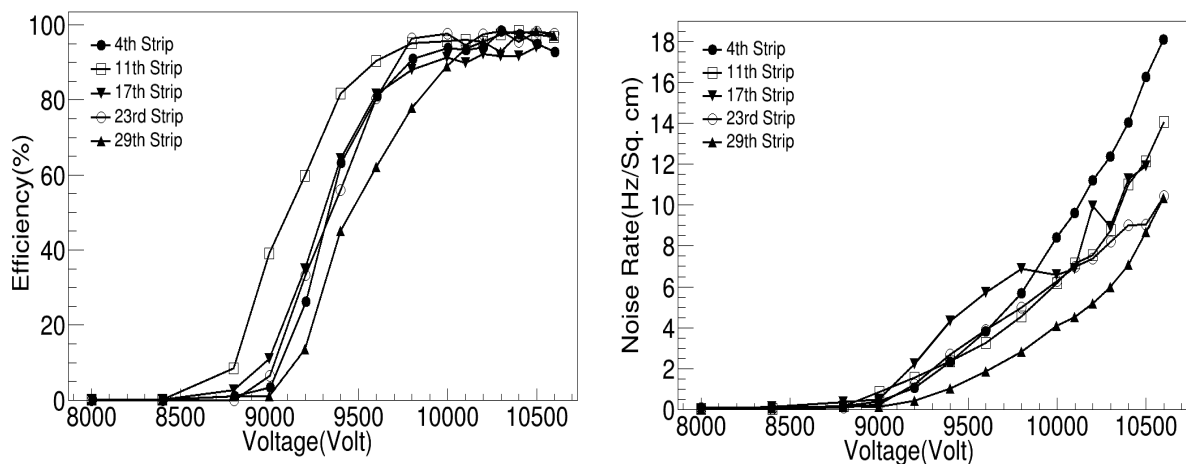


Figure 12: Efficiency vs. voltage characteristics (left), noise rate vs. voltage characteristics (right) for 5 different RPC strips for the 1<sup>st</sup> gas composition.

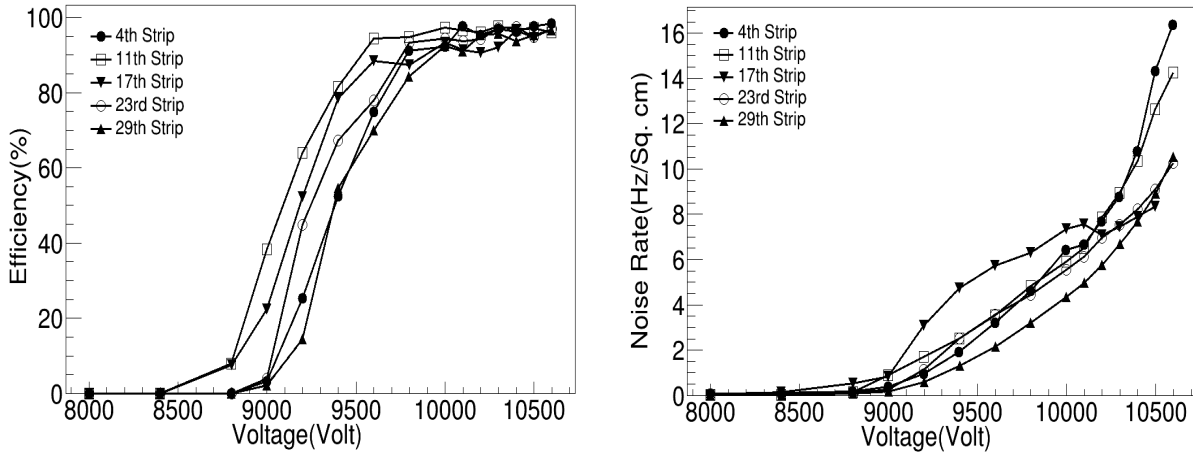


Figure 13: Efficiency vs. voltage characteristics (left), noise rate vs. voltage characteristics (right) for 5 different RPC strips for the 2<sup>nd</sup> gas composition.

## 5. Conclusions

The presented work establishes the operating parameters for the glass based RPC for different gas compositions. We have performed the leakage current studies for varying gas compositions, the pulse width optimization using the optimized gas composition, the efficiency and noise rate studies for the fixed gas flow rate keeping the temperature and relative humidity controlled throughout the measurements. We have also performed the efficiency and noise rate studies at 5 different locations on the RPC with the same set of parameters. From the leakage current, efficiency and noise rate studies, it is concluded that the glass RPC gives the best performance for the 1<sup>st</sup> gas composition. The efficiency and noise rate characteristics have been found to be uniform throughout the RPC.

## Acknowledgements

We would like to thank Department of Science and Technology (DST) and Department of Atomic Energy (DAE)/Govt. of India for providing the financial support to accomplish this work. We would also like to acknowledge the help of other INO collaborators in procuring some of the raw materials for the detector assembly.

## References

- [1] The ICAL Collaboration et al., Physics Potential of the ICAL detector at the India-based Neutrino Observatory (INO), arXiv: 1505.07380v1, 2015.
- [2] S. Bhide et al., Preliminary results from India-based Neutrino Observatory detector R&D programme, *Journal of Physics*, 69(6) (2007) 1015-1023.
- [3] Srubabati Goswami, Physics program of the India-based Neutrino Observatory, *Nucl. Phys. Proc. Suppl.* 188(2009) 198-200.
- [4] R.N. Mohapatra et al., Theory of Neutrinos : A White Paper, *Rept.Prog.Phys.*70:1757-1867,2007.
- [5] G. Aielli, R. Santonico et al., *Nucl. Instr. and Meth.* 187 (1981) 377.
- [6] S.D.Kalmani et al., Development of glass Resistive Plate Chambers for INO experiment, *NIM A* 602(2009).
- [7] A. Mengucci et al., *NIM A* 583(2007).
- [8] W.R. Leo, *Techniques for Nuclear and Particle Physics Experiments*, 2<sup>nd</sup> Revised Edition, Springer Publication (1994).